

See discussions, stats, and author profiles for this publication at: <https://www.researchgate.net/publication/323774075>

Observed and modelled temperature and precipitation extremes over Southeast Asia from 1972 to 2010

Article in *International Journal of Climatology* · March 2018

DOI: 10.1002/joc.5479

CITATION

1

READS

146

10 authors, including:



Bertrand Timbal

National Environment Agency

95 PUBLICATIONS 4,385 CITATIONS

[SEE PROFILE](#)



Nicola Golding

Met Office

21 PUBLICATIONS 232 CITATIONS

[SEE PROFILE](#)



Boonlert Archevarahuprok

Thai Meteorological Department

17 PUBLICATIONS 13 CITATIONS

[SEE PROFILE](#)



Dodo Gunawan

Meteorological Climatological and Geophysical Agency

30 PUBLICATIONS 720 CITATIONS

[SEE PROFILE](#)

Some of the authors of this publication are also working on these related projects:



Climate Change Impacts on the Australian Sugarcane Industry [View project](#)



Scale interactions over southeast Asia [View project](#)

RESEARCH ARTICLE

Observed and modelled temperature and precipitation extremes over Southeast Asia from 1972 to 2010

W. K. Cheong¹ | B. Timbal¹  | N. Golding² | S. Sirabaha³ | K. F. Kwan⁴ | T. A. Cinco⁵ | B. Archevarahuprok⁶ | V. H. Vo⁷ | D. Gunawan⁸ | S. Han⁹

¹Meteorological Service, Singapore, Singapore

²Hadley Centre, Met Office, Exeter, UK

³Brunei Meteorological Service, Department of Civil Aviation, Bandar Seri Begawan, Brunei Darussalam

⁴Malaysian Meteorological Department, Kuala Lumpur, Malaysia

⁵Department of Science and Technology, Philippine Atmospheric, Geophysical and Astronomical Services Administration, Diliman Quezon City, Philippines

⁶Thai Meteorological Department, Bangkok, Thailand

⁷National Weather Forecasting Center, Hanoi, Vietnam

⁸Meteorological and Geophysical Agency, Jakarta, Indonesia

⁹Department of Meteorology and Hydrology, Naypyidaw, Myanmar

Correspondence

B. Timbal, Centre for Climate Research Singapore, Meteorological Service Singapore, 36 Kim Chuan Road, Singapore 537054. Email: bertrand_timbal@nea.gov.sg

Funding information

National Environment Agency (NEA) Singapore

Regional assessments of trends in climate extremes are necessary for countries to make informed decisions about adaptation strategies and to put these changes into a global context. A workshop bringing together several Southeast Asian countries has delivered a new set of daily weather observations suitable to analyse the changes in temperature and precipitation extremes between 1972 and 2010. The use of a consistent and widely tested methodology in this study allows a direct comparison with results from other parts of the world. Trends in a range of climate extremes indices were assessed focusing on spatial variation in these trends. For most locations temperature trends obtained in this study appear broadly consistent with previous assessments; for some locations stronger trends have been detected through the inclusion of new data. In contrast to earlier studies, evidence of trends in precipitation extremes is emerging, with significant increasing trends in both regional and subregional data. In addition, large correlations between regional rainfall extremes and large-scale features such as El Niño-Southern Oscillation and the Indian Ocean Dipole were identified. Finally, the observed trends are compared with a regional climate model reconstruction of the historical period. It was found that the model captures very well the trends and spatial variation of temperature extremes across the region, albeit with an underestimation of the more extreme indices. In contrast, the trends in precipitation extremes are largely overestimated, particularly in the western side of Southeast Asia.

KEYWORDS

climate model evaluation, observations, rainfall extremes, Southeast Asia, temperature extremes

1 | INTRODUCTION

Extreme climate events such as droughts, intense rainfall and prolonged high temperatures are known to have high social, economic and ecological impact (Intergovernmental Panel on Climate Change, 2012). In addition, it is expected that any future changes in extreme events will have greater negative impacts on these systems than changes in the mean climate (Katz and Brown, 1992; Choi *et al.*, 2009). In recent years there has been an observed increase in extreme events

in many parts of the world (Manton *et al.*, 2001; Alexander and Arblaster, 2009). However, whether this is due to global warming, to shorter-term natural variations in the Earth's climate or to human factors such as increasing populations in vulnerable locations is unclear.

Changes to the mean state of the climate over the past century, and in particular over the past 50 years, have been well documented and global and regional trends are fairly well established (Intergovernmental Panel on Climate Change, 2007, 2013). However, analysing observed changes

in extreme precipitation and temperature is a much more recent development due to difficulties in collecting the high spatial and temporal resolution climate data necessary for these studies. In addition, there are currently large areas of the world with sparse data coverage, which makes analysis of low-frequency climate events problematic and prevents the quantification of trends in extreme events over the 20th century (Easterling *et al.*, 1999).

The Intergovernmental Panel on Climate Change (IPCC) Fourth Assessment Report greatly benefitted from an international effort to improve this situation through a series of workshops (Peterson and Manton, 2008) coordinated by the Expert Team on Climate Change Detection and Indices (ETCCDI) which is sponsored by the World Meteorological Organisation (WMO) Commission for Climatology, the Joint Commission for Oceanography and Marine Meteorology (JCOMM) and the Research Programme on Climate Variability and Predictability (CLIVAR). The ETCCDI workshops aim to gather participants from countries within a data-sparse region to improve the data record and enhance capability. Previous workshops in the Southeast Asia (SEA) region have been held in 1998, 1999 (Manton *et al.*, 2001) and again in 2007 (Caesar *et al.*, 2011). Results from these workshops showed strong and consistent trends in temperature, with particular increases in the frequency of warm nights (Manton *et al.*, 2001), and faster reductions in cold days and cold nights. Precipitation trends were much harder to interpret, and few significant trends were identified at a regional scale.

As a basis for the present work, workshops were held in Singapore in May 2011 and June 2012 with participants from across SEA. The workshops aimed to update previous records with new station data and improved quality records and also to investigate some features in more detail. One objective of this work was to consider the relationship between station trends and the internal variability modes of the El Niño-Southern Oscillation (ENSO) and the Indian Ocean Dipole (IOD). These relationships were investigated globally by Kenyon and Hegerl (2008; 2010), who found that ENSO showed a particularly clear influence on extremes around the Pacific Rim. Similarly, Alexander *et al.* (2009) found that global sea surface temperature anomaly patterns influence the modulation of extreme temperature and precipitation around the globe. In general, prolonged drought conditions in SEA are associated with El Niño while severe floods tend to be associated with La Niña. However, previous studies have shown considerable spatial and strong seasonal variation in these relationships (Nicholls, 1981; Chang *et al.*, 2003; Tangang and Juneng, 2004). The variability in landfall of tropical cyclones in the region is particularly dependant on the phase of ENSO (Liu and Chan, 2003; Goh and Chan, 2010). In addition to ENSO, the IOD is known to drive climate variability in SEA, although the mechanisms by which this occurs are

less well understood. The IOD is generally associated with temperature and rainfall variability in two modes, whereby one causes anomalously low rainfall over countries on the eastern rim of the Indian Ocean, and the other causes enhanced rainfall over the Asian monsoon trough (Saji and Yamagata, 2003). Here we investigate further the regional and subregional influences of both ENSO and the IOD, and the evidence for relationships with the extremes observed in the data. Any strong correlations here will have implications for the predictability of extremes in the region and therefore are of significance to modellers and ultimately decision makers.

Climate models are now being used to project potential changes to extreme events in many regions of the world. Studies comparing model results to the observational record have long suggested that models do not represent well the occurrence of climatic extremes and therefore add considerable uncertainty to future projections (e.g., Meehl *et al.*, 2007; Sillman and Roeckner, 2008; Alexander and Arblaster, 2009), although more recent studies have pointed to model achieving a similar degree of uncertainty in past climate model simulations than in observations (Gervais *et al.*, 2014; Alexander and Arblaster, 2017). Global climate models are unable to simulate realistically the variability of the climate and in particular extreme climate events due to their coarse resolution as compared to the scales on which many events occur (particularly precipitation extremes). Therefore, as part of this study we use a regional climate model (RCM) to downscale the modelled climate to a more suitable resolution of 25 km. We compare the observational record with the results from a reanalysis data-driven RCM experiment in order to question how realistic the additional detail from downscaling is.

In this article, we begin by describing the daily climate data gathered at the 2011 and 2012 workshops and methods used (section 2) before describing results (section 3) from both the station data and comparison with large-scale modes of variability and the model. We then discuss the relevance of this study (section 4).

2 | DATA AND METHODS

2.1 | Station data

Invitation were sent to all countries within the ASEAN region (Association of Southeast Asian Nations, a geopolitical and economic organisation of countries) to contribute to this study. A total of 146 stations of climate indices were received from 8 out of 10 ASEAN countries: Brunei, Indonesia, Malaysia, Myanmar, Philippines, Singapore, Thailand and Vietnam. Some indices, such as the 90th percentile of daily T_{\max} (TX90p), require a base period over which to compute them. The period of 1972–2010 was used in this

study as a baseline for all stations where the data covered this period. The station data supplied by Indonesia and Myanmar did not cover the entire base period and therefore were not considered. In this study we present the regional climate indices, computed using daily time series of temperature (maximum and minimum) and precipitation for a total of 121 stations from six countries (Brunei, Malaysia, Philippines, Singapore, Thailand and Vietnam; shown in Figure 1). Data supplied included daily maximum and minimum temperatures, and daily precipitation totals. Data from individual countries can be accessed by direct request to the relevant National Meteorological Service.

All data used in the study have been quality controlled using the procedures in the RClimDex software (the RClimDex packages can be downloaded from the ETCCDI website <http://cccma.seos.uvic.ca/ETCCDI/>); the quality control was conducted by each individual country and evaluated during the workshop to ensure consistency across the region. Errors such as negative daily precipitation amounts due to manual keying errors were removed and both daily maximum and minimum temperatures set to a missing value if daily maximum temperature is less than daily minimum temperature. In this study, outliers are defined as lying outside four standard deviations (*SD*) from the climatological mean of the value for the day, that is, $\text{mean} \pm 4 \text{ SD}$. Daily temperature values outside of this range were manually checked and edited on a case by case basis by authors who are knowledgeable about their own daily data.

Unlike many previous regional indices workshops, where final quality control and indices processing for all stations from the regions was completed centrally, this study took the approach of having the quality control performed independently by scientists in each of the participating countries. A set of uniform guidelines was supplied to each participant, and efforts were made to ensure objective decisions on data quality were made consistently. Part of the

workshop process was to identify whether any results may have been influenced by this process and stations with questionable quality were removed. Following quality control, the extremes indices were calculated using RClimDex before being collated for this study. In term of data completeness, to be considered in this study, any stations had to have less than 20% of the missing data in any given year during the analysis period.

The stations were divided into four climatically similar subregions: northwestern (NW), southwestern (SW), northeastern (NE) and southeastern (SE) (Figure 1). SEA as a whole has a more homogeneous climate than the larger regions considered previously (Manton *et al.*, 2001; Caesar *et al.*, 2011); however, there are key subregional differences which are usefully delineated here. Data from all available stations were combined to produce regional and subregional mean time series for each index.

SEA is under the influence of monsoon winds of seasonal character. The northeast monsoon affects the region from October to February, and the southwest monsoon from May to October. Tropical storms also have direct impacts on the weather conditions over NW and NE. NW is affected by only about three to four tropical storms a year, while a large proportion of the rainfall over NE is due to the influence of tropical storms. Tropical storms do not affect directly SE, and only minimal and indirect effects are felt (Chan, 2005).

There is a relatively large seasonal variation of temperatures over NW. The maximum temperatures usually reach near 40 °C and temperatures may be near or below 0 °C in winter at high-elevation locations. Temperatures over SE and SW are far more uniform throughout the year because of the maritime and tropical characteristics of this region. The characteristic features of the climate over SE and SW are uniform temperature, high humidity and copious rainfall. There is no distinct wet or dry season, but rainfall is

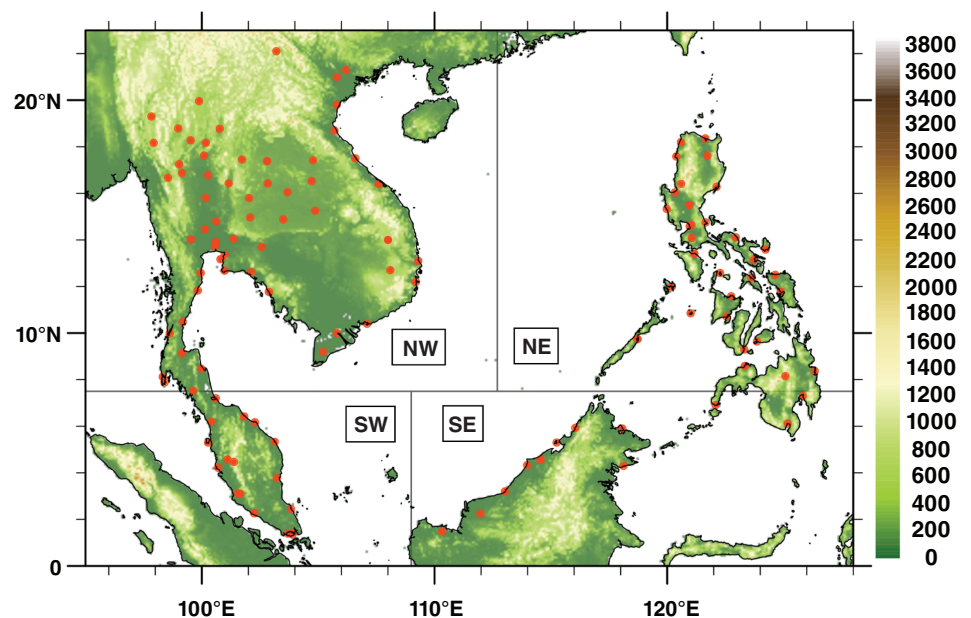


FIGURE 1 Location of the 121 stations assessed for this study and the limits of the four subregions. Background is the region orography

TABLE 1 Climate indices computed as part of this study

Index	Indicator name	Units
TX90p	Warm days (above the 90th percentile)	Percentage of days
TX10p	Cool days (below the 10th percentile)	Percentage of days
TN90p	Warm nights (above the 90th percentile)	Percentage of days
TN10p	Cool nights (below the 10th percentile)	Percentage of days
TXx	Max T_{\max}	°C
TXn	Min T_{\max}	°C
TNx	Max T_{\min}	°C
TNn	Min T_{\min}	°C
DTR	Diurnal temperature range	°C
PRCPTOT	Annual total wet-day precipitation	mm
SDII	Simple daily intensity index (average rainfall on days with ≥ 1 mm rain)	mm/day
CDD	Consecutive dry days (days with ≤ 1 mm rain)	Days
CWD	Consecutive wet days (days with ≥ 1 mm rain)	Days
RX5day	Maximum 5-day precipitation	mm
RX1day	Maximum daily precipitation	mm
R99p	Precipitation total due to extremely wet days (above the 99th percentile of days with ≥ 1 mm rain)	mm
R95p	Precipitation total due to very wet days (above the 95th percentile of days with ≥ 1 mm rain)	mm
R40mm	Extremely heavy precipitation days (≥ 40 mm)	Days
R20mm	Heavy precipitation days (≥ 20 mm)	Days

characterized by high intensities (measured in mm/hr) due to small to mesoscale convection cells of thunderstorms and squall lines.

2.2 | Indices

A total of 27 indices, based upon recommendations of the ETCCDI, were calculated using RCLIMDEX. The ETCCDI website lists the complete set of indices and their definitions, and Table 1 lists the indices presented in this study. Monthly indices were computed, from which seasonal or annual indices were derived. Discussions were held at the workshop to assess how useful the available indices were to users, and this informed the selection in Table 1. In addition, threshold measures were adapted to reflect the climate of the region, for instance R10mm was not considered “heavy rain” by the participants so R20mm was chosen instead. Absolute value thresholds were preferred to characterize extreme rainfall events instead of percentiles-based one for their simplicity and common understanding.

2.3 | Trend calculation and regional series

Ordinary least squares method was used to calculate the trends of the indices. Caesar *et al.* (2011) indicated that a simple least squares method might not be appropriate for indices data that do not follow a Gaussian distribution. To investigate the appropriateness in using least squares method in computing the trends, a comparison was made between the least squares estimator and Kendall’s slope estimator used for the same purpose by Caesar *et al.* (2011). In general, statistically significant trends in the indices were

consistently identified by both approaches. Regional (and subregional) linear trends averaged across the weather stations were computed to examine the overall trends across SEA. In averaging the trends, however, no area-based weighting corrections are made, so areas with a high data density will be over-represented in the regional averages. Thus, spatial maps of the trends at individual weather stations are also provided in this study. In this study, a trend is considered to be statistically significant if it is significant at the 5% level.

2.4 | Relationships between extreme indices and large-scale atmospheric phenomenon

To investigate the relationship between the extreme indices and large-scale atmospheric phenomena such as the ENSO and IOD, we computed the Pearson product–moment correlation between the indices and the Southern Oscillation Index (SOI) and Dipole Mode Index (DMI).

The SOI is calculated using the pressure differences between Tahiti and Darwin and gives an indication of the development and intensity of El Niño or La Niña events in the Pacific Ocean (SOI is available from the NOAA Climate Prediction Center website (<http://www.cpc.ncep.noaa.gov/data/indices/soi>)). Sustained negative values of the SOI often indicate an El Niño episode; sustained positive values of the SOI are typical of a La Niña event. In view that May and June often represent a time of the year of transition of the ENSO state, that is, when ENSO episodes are ending or new episodes are just beginning to grow (Webster and Yang, 1992; Ju and Slingo, 1995; Turner *et al.*, 2005), the relationship between the indices and SOI anomalies, on an

annual basis, was investigated based on the averages of the indices between July and the following June.

The intensity of the IOD is represented by anomalous SST gradient between the western equatorial Indian Ocean (50°–70°E, 10°S–10°N) and the southeastern equatorial Indian Ocean (90°–110°E, 10°S–0°N); this gradient is named as the DMI. During a positive IOD year, the eastern Indian Ocean is colder than normal while the western Indian Ocean is warmer than normal. Because the DMI is defined as a difference between the western and the eastern Indian Ocean, DMI is positive during a positive IOD year and vice versa. DMI data up to September 2010 are available from the Japan Agency for Marine-Earth Science and Technology http://www.jamstec.go.jp/frcgc/research/d1/iod/DATA/dmi_HadISST.txt.

2.5 | Model comparison

We ran the 25-km resolution RCM HadRM3P (Jones *et al.*, 2004) driven by ERA40 reanalysis data (Uppala *et al.*, 2005) over the study region within a spatial domain from 90° to 135°E and 28°N to 10°S. This area was selected to encompass as much of the ASEAN region as possible and capture important regional climatic features while maintaining a manageable size appropriate for running an RCM of this resolution (for more discussion on the appropriate selection of domain size for RCM experiments, see Bhaskaran *et al.*, 1996). Initial conditions were taken from ERA-40 instantaneous 3D assimilation for the day and time at the start of the RCM integrations. The model has 19 vertical levels and 5-min time steps; the full model setup can be accessed from the PRECIS website and technical report (Wilson *et al.*, 2015). The model has proven useful in reproducing regional climate and has been used extensively across the ASEAN region to study regional impacts of climate change (e.g., change in tropical cyclone over Vietnam (Redmond *et al.*, 2015) or change in rainfall over Malaysia (Loh *et al.*, 2016). No specific simulation was run for this study, instead it was decided to make use of an existing simulation which was run from 1959 to 2002 and therefore overlaps most of the observational data time series (results from this simulation were incomplete for the year 1992 which is therefore omitted in the result section). For calculation of trends requiring a baseline period, we recalculated the station data trends to use the same baseline of 1972–2001 for comparison purposes. A single RCM simulation was available, preventing any possibility to assess internally generated variability.

The grid boxes containing each of the station points used in this study were then extracted to form time series equivalent to those for each station. These were then used to calculate indices (see method above) and combined to produce regional and subregional model mean time series for each index. By using this method, we ensure that only the areas where station data are available were sampled

from the model. However, this raises the issue of comparing point data (e.g., the stations) with smoothed model grid boxes, which will undoubtedly impact the comparison of extreme values. For instance, we would expect the model to consistently underestimate the tails of a distribution as the values are averaged over an area, rather than recording the highest value at a point. For regions where high-resolution gridded daily data products are available (e.g., the European E-OBS data set) (Haylock *et al.*, 2008), a more complete validation of modelled extremes can be attempted (see, e.g., Herrera *et al.*, 2010). However, in many regions of the world, including much of the study region used here, sparse and incomplete data records make this unsuitable. For this reason, while we do calculate correlations between station data and model values, we focus more on whether the spatial and temporal trends are represented adequately in the model; furthermore, results are evaluated at the subregional level to limit the pertinence of this limitation. The influence of station density on the evaluation of gridded data from RCMs is discussed more thoroughly in Hofstra *et al.* (2009).

3 | RESULTS

3.1 | Trends in temperature indices

Initially, we considered trends in four percentile-based temperature indices (the 10th and 90th percentile of both daily maximum and minimum temperature) at individual stations. These are compared to examine the extent to which the magnitudes of their changes are consistent with the region as a whole. We find there is a statistically significant upwards trend in the occurrence of warm days for 55% of the stations (Figure 2 top left; $p < .05$ for the remainder of the article). Of those stations indicating significant upwards trends, half of them indicate an increase of more than 5%/decade in the number of warm days. A similar increase in warm nights is also detected across the region (Figure 2, bottom left). Fifty-four percent of stations show statistically significant decreasing trends in the occurrence of cool days (Figure 2, top right). For two stations there is a greater than 5% decrease in cool days.

Of the indices considered, the frequency of warm and cool nights (TN90p and TN10p) show the most consistent pattern with large areas showing strong increasing and decreasing trends, respectively (Figures 2, right). Eighty percent of the stations show statistically significant upwards trends in the occurrence of warm nights. Seventy-nine percent of the stations show significant downwards trends in cool night's occurrence. In contrast to daytime temperatures, these results show evidence of a greater decrease in cool nights than the equivalent increase in warm nights. This is in agreement with previous literature (Caesar *et al.*, 2011). The consistency of trends in night-time temperature also

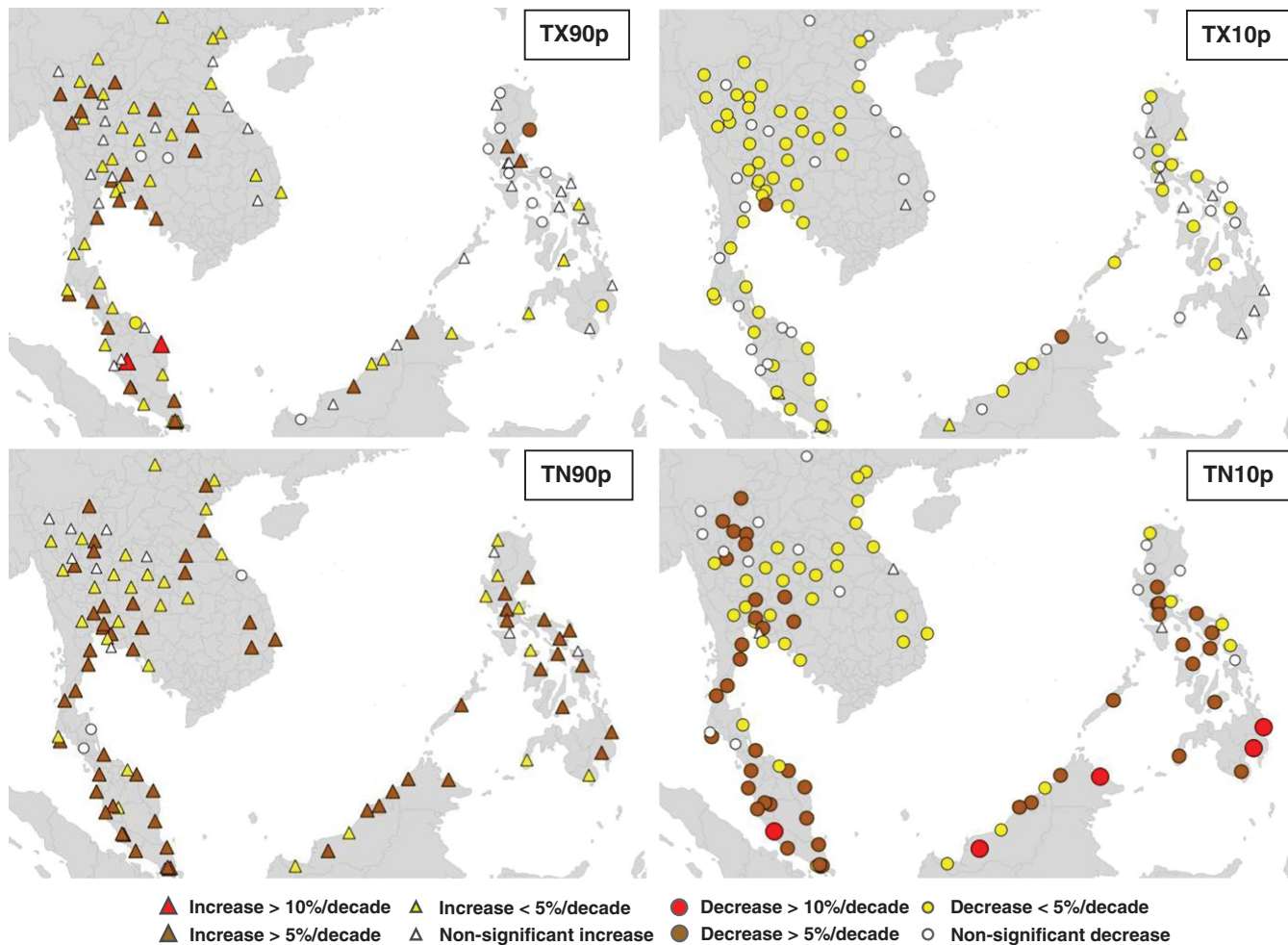


FIGURE 2 Station trends for percentage of (top left) warm days, cool days (top right), warm nights (bottom left) and cool nights (bottom right) for the period 1972–2010. In all charts, positive trends are represented by triangles, negative trends by circles. Symbol size and colour are proportional to the magnitude of the trend. Coloured (white) symbols indicate trends significant (non-significant) at the 5% level, respectively

suggests that there is limited effect from the urban environment.

Figure 3 shows regional and subregional mean time series for warm days (TX90p). All subregions, except NE, show significant ($p < .05$) increments in the number of warm days between 1972 and 2010. The regional and subregional series display annual peaks coincident with El Niño episodes; in particular, 1998 stands out. NE appears to lack

the increasing trend as evident in other subregions, particularly in the last decade. It is observed that NE and SE show weaker trends than SW and NW. One possible reason is the moderating effect of the large ocean surrounding the Philippines and eastern Malaysia on the local signature of global warming.

Table 2 lists the regional and subregional trends for all the temperature indices examined in this article. When averaged over the region, almost all of the temperature indices show significant changes over the 1972–2010 period. For the percentile-based indices, we see general agreement in the sign and significance of trends in all regions, except for a non-significant upwards trend in the occurrence of warm days over NE. In general, over the entire region, the frequency of warm nights has increased and the frequency of cold days and nights has decreased.

Trends in absolute temperature indices (TXx, TXn, TNx, TNn and DTR) reflect significant increasing trends in both the maximum and minimum annual daily minimum temperatures (TNx and TNn). Trends for annual maximum daily maximum temperature (TXx) are generally non-significant over the region with an exception over SW which showed a

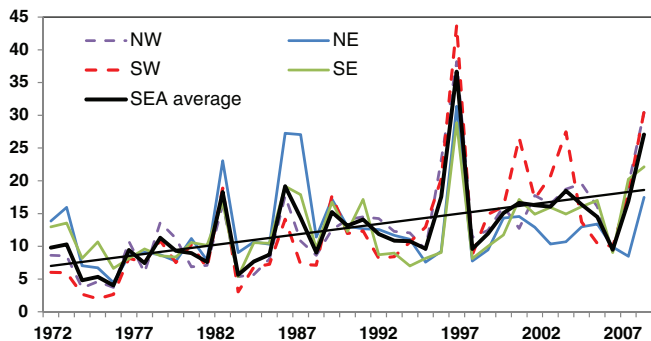


FIGURE 3 Regional and subregional time series for TX90p (units: %) for SEA average and subregions. Straight line indicates ordinary least squares fit based on SEA average

TABLE 2 Trends in temperature indices for the period 1972–2010; trends significant at the 5% level are highlighted in bold

Index	SEA	NW	NE	SE	SW	Units/decade
TX90p	3.05	3.80	0.72	1.81	4.63	Percentage of days
TX10p	-1.82	-2.31	-1.11	-1.03	-2.12	Percentage of days
TN90p	4.82	4.41	3.72	5.31	6.63	Percentage of days
TN10p	-4.91	-3.70	-4.2	-6.71	-6.82	Percentage of days
TXx	0.09	0.08	0.002	-0.01	0.20	°C
TXn	0.16	0.18	0.20	0.08	0.16	°C
TNx	0.18	0.14	0.11	0.16	0.29	°C
TNn	0.60	0.79	0.49	0.45	0.53	°C
DTR	-0.11	-0.07	-0.16	-0.2	-0.14	°C

significant rate of increase of 0.2 °C/decade. The magnitude of the trends is also generally greater for minimum temperature (TXn and TNn) related extremes. Annually, the largest change in extremes corresponding to an increase in minimum daily minimum temperature is 0.79 °C/decade over NW.

These results are largely in agreement with those found by Caesar *et al.* (2011) in a previous study for SEA, with minimum temperatures showing a stronger increase than maximum temperatures (thereby reducing DTR). Some indices show much higher trends, however, with night-time indices (TN90p and TN10p) approximately double the previous estimate, possibly suggesting a sharp increase of trends in the recent decade. We find that on the whole trends are strongest in SW and weakest in SE and NE as previously discussed. It is also important to note that there are fewer stations in the SW and SE and therefore trends are likely to be more skewed by the data from one station.

The decadal trends for the seasonal occurrence of warm days and nights are shown in Table 3. Warming is observed in all seasons, and in particular it is noted that significant night-time warming trends are observed in all seasons and all subregions. The largest changes in night-time temperatures are found in DJF. In all seasons and for both indices, we see a significant warming over SW. There is no significant change in the occurrence of warm days over NE for 1972–2010 periods in all seasons. For MAM there is no significant change over SEA or the subregions, except for SW.

3.2 | Trends in precipitation indices

There is a relative lack of spatial coherence of trends in the precipitation indices (Figure 4). We observe only 16 and 13% of the stations showing statistically significant (p

< .05) upwards trends in the annual total wet-day precipitation (PRCPTOT) and R95p index, respectively. Less than 3% of the stations (3 out of 121) indicate significant downwards trends in both precipitation indices. Figure 4 (bottom) shows that the number of stations with significant trends in either direction is low for the maximum daily precipitation amount (RX1day); only eight and four of the stations show significant upwards and downwards trends, respectively.

The trends found in this study, particularly increases in RX1day in the Philippines and central Vietnam, are quite large in some locations but lack spatial coherence and may be related to trends in tropical cyclone activities in the region (for further discussion see, e.g., Chan and Shi, 1996; Ho *et al.*, 2004; Liu and Chan, 2008). Significant trends also stand out on the Malay Peninsula and Singapore.

The regional and subregional trends for all the precipitation indices examined in this article are listed in Table 4. The regional time series for the fractional contribution to the annual total precipitation due to very wet days (R95p) (Table 4) show a statistically significant upwards trend as well as but this is limited to NW and SW. We find a general increase in precipitation indices, except for consecutive dry days (CDD) and consecutive wet days (CWD) for which trends are not statistically significant (as well as RX5day, RX1day and R99p). When compared with temperature changes, we see a less spatially coherent pattern of statistical significance changes. However, there are significant regional trends (PRCPTOT, SDII, R95p R40mm and R20mm) that have not been found in previous studies.

Over the equatorial subregions (SE and SW), we see a significant increase in both of the frequency-based precipitation indices, that is, the R40mm and R20mm indices. There is also a significant increase in the annual total wet-day

TABLE 3 Seasonal trends in warm days (WD) and warm nights (WN) for the period 1972–2010 expressed as percentage of days/decade; trends significant at the 5% level are highlighted in bold

Season	SEA WD/WN	NW WD/WN	NE WD/WN	SE WD/WN	SW WD/WN
DJF	4.8/8.3	6.0/9.0	2.3/5.1	1.9/8.2	6.8/10.5
MAM	1.9/6.6	2.5/5.4	0.3/5.8	1.8/7.0	4.1/9.3
JJA	3.1/6.3	4.5/6.5	1.3/4.4	3.1/7.4	4.7/8.4
SON	4.6/6.8	6.6/6.3	1.0/4.6	2.3/7.3	6.1/9.6

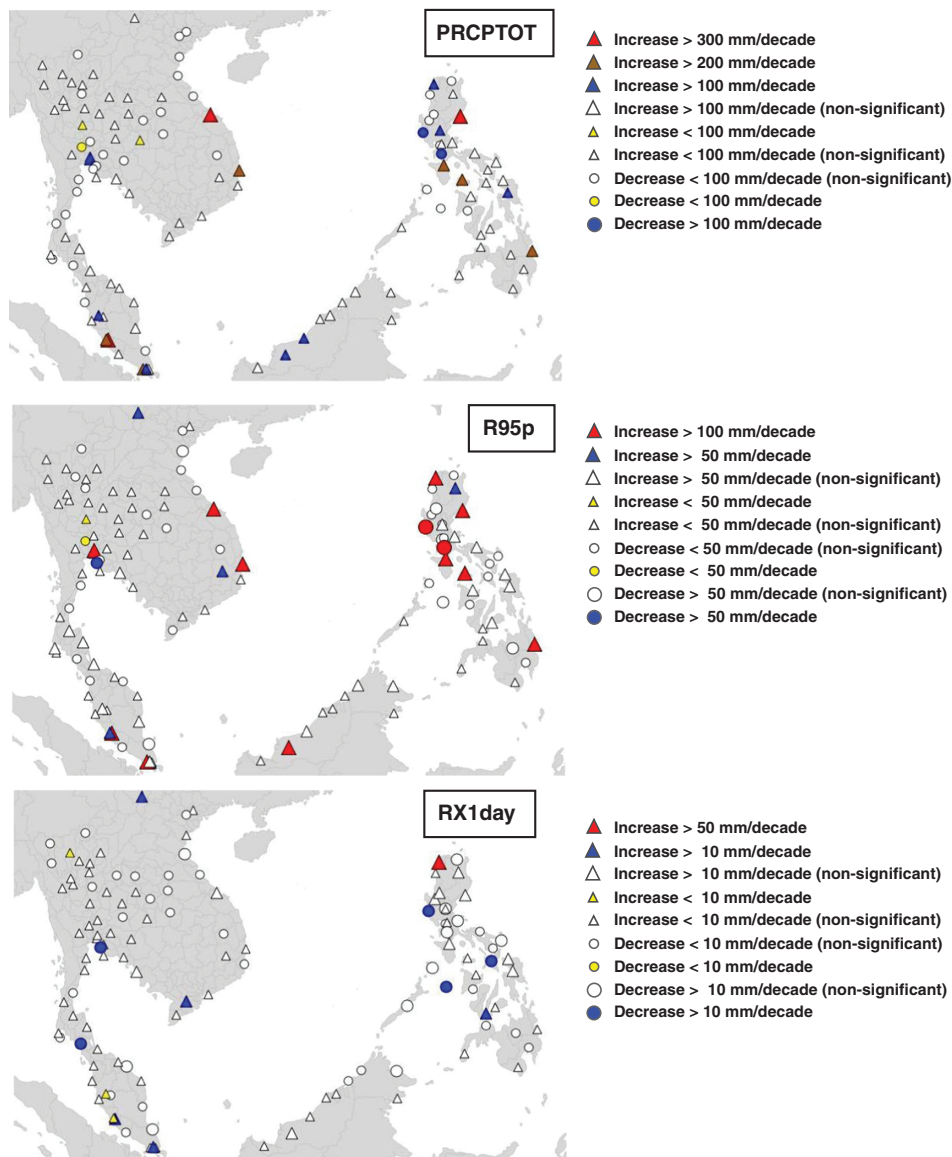


FIGURE 4 Station trends for annual total wet-day precipitation (top), precipitation total due to very wet days (middle) and annual max daily total precipitation (bottom) for the period 1972–2010. Coloured (white) symbols indicate trends significant (non-significant) at the 5% level, respectively

TABLE 4 Trends in precipitation indices for the period 1972–2010; trends significant at the 5% level are highlighted in bold

Index	SEA	NW	NE	SE	SW	Units/decade
PRCPTOT	59.6	27.2	49.6	88.1	123.3	mm
SDII	0.2	0.3	−0.02	0.3	0.3	mm/day
CDD	−1.8	−2.2	−1.3	−1	−1.3	Days
CWD	−0.08	−0.01	−0.30	0.01	−0.06	Days
RX5day	2.3	2.7	2.3	2.1	−1	mm
RX1day	1.6	2.4	−1.3	0.8	2.1	mm
R99p	0.002	0.002	−0.001	0.003	0.004	mm
R95p	0.006	0.007	0.0002	0.004	0.009	mm
R40mm	0.5	3.2	0.5	0.9	0.7	Days
R20mm	1	0.5	1	1.8	1.4	Days

precipitation (PRCPTOT) and the average rainfall on days with ≥ 1 mm rain (simple daily intensity index [SDII]). Northern subregions show few significant changes in precipitation indices.

In most seasons, there is an increase in the annual maximum daily rainfall total (RX1day) over the region as a

whole (Table 5). There is an exception of decreasing trends in this index over SE in June–August; however, we note that these trends are non-significant. In contrast to the temperature changes, there are very few areas of significant change in precipitation. We observed only significant increases in RX1day over the NW in MAM and over SW

TABLE 5 Seasonal trends in annual maximum daily rainfall total (RX1day) for the period 1972–2010; trends significant at the 5% level are highlighted in bold

Season	SEA	NW	NE	SE	SW	Units/decade
DJF	2.9	1.2	4.7	3.1	4.6	mm
MAM	3.3	3.2	5.2	2.5	2.2	mm
JJA	1.5	1.2	-0.2	3.3	2.7	mm
SON	1.0	0.6	3.2	-0.2	0.7	mm

and SE in June–August (Table 5). There is no significant change in the maximum daily rainfall over NE in any seasons.

3.3 | Relationship with ENSO and IOD

The ENSO and IOD are two dominant modes of climate variability in the tropical Pacific and Indian Oceans. Both modes are shown to influence the climatic conditions of several parts of the world (Diaz *et al.*, 2001; Saji and Yamagata, 2003). Being located in between those two basins, climates in SEA are expected to be influenced by both phenomena. In this study, we investigate the influences on extremes indices arising from different phases of ENSO and IOD and consider how the relationships evidenced here support our existing understanding of how these phenomena affect both mean and extreme climates in the region (Alexander *et al.*, 2006; Kenyon and Hegerl, 2008; 2010). It is well recognized in the literature that the two phenomena investigated here are significantly correlated (Allan *et al.*, 2001; Behera *et al.*, 2005), and this should be appreciated when considering relative relationships between each and the trends in extreme temperature and rainfall in the region. Correlations were computed for all indices considered in this study. For the sake of brevity only the most significant correlations observed are reported in the following section; in this section only correlations of magnitude larger than .3 are significant at the 5% level.

3.3.1 | Relationship with SOI

The correlation map between TN90p and SOI anomalies shows a cluster of relatively strong ($-0.2 < \rho < -0.6$) negative correlation over NW, SW and SE (Figure 5), indicating that an increase in the number of warm nights can be expected with El Niño episodes. This relationship holds true for other temperature indices and is in agreement with the literature (Caesar *et al.*, 2011), supporting the driving mechanisms of variability previously identified. We see more mixed signals over NE and the Philippines as a whole, with more positive correlations in evidence around the northern islands.

The seasonality of ENSO is such that it is expected to have greatest influence in this region in December–February. In all seasons except September–November (SON) negative correlations are noted over the equatorial part of the southern subregions (not shown). Over these

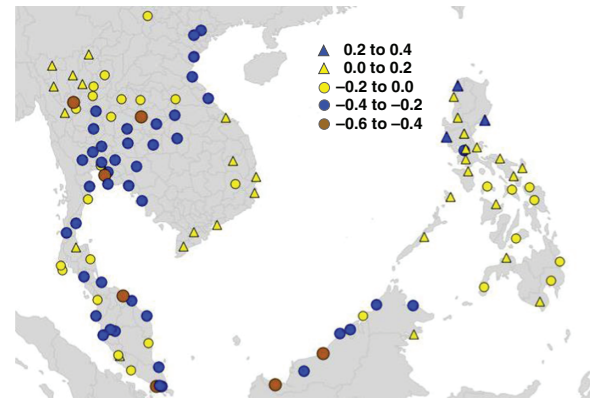


FIGURE 5 Correlation between annual mean (from July to June) of TN90p and the SOI

subregions, the strongest negative correlation is noted during the winter monsoon period (DJF), that is, a very high possibility for an increase in the frequency of warm nights over the equatorial region is expected with El Niño episodes during this season (not shown). In the northern subregions (NW and NE), positive relationships are evident during DJF which indicates an increase in the frequency of warm nights over this region may be expected with La Niña episodes. Over NW, we generally observe mixed relationships throughout the seasons, although more negative relationships are evident during the March–May season. Regionally, the frequency of warm nights is less influenced by ENSO episodes during the SON season.

The correlation pattern between RX1day and SOI anomalies (Figure 6) highlights the strong relationship between rainfall and ENSO over NE and SE. Strong ($\rho > .6$) positive correlation (i.e., an increase in the maximum daily precipitation amount with La Niña episode) is evident over NE. NW and SW indicate relatively weaker correlations ($\rho < .6$) between the variables and the relationship also weakens towards the equator. Again, the results found here

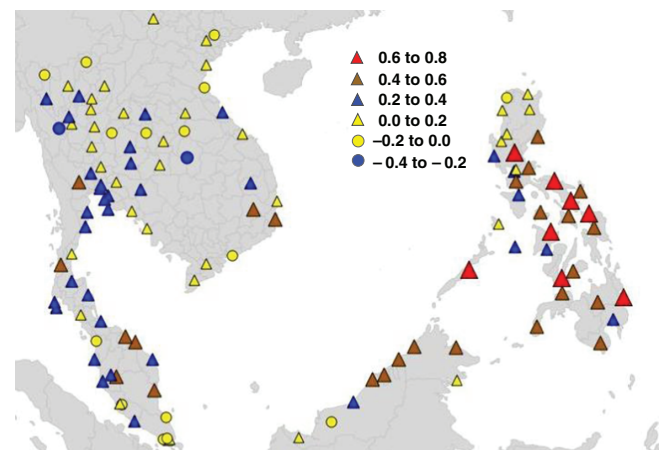


FIGURE 6 Correlation between annual mean (from July to June) of RX1day and the SOI

support the existing literature and understanding of ENSO teleconnections in this region (Caesar *et al.*, 2011). The strong response over the Philippines in RX1day also concurs with the expectation that tropical cyclone activity will increase in La Niña episodes.

At the seasonal timescale (not shown), stronger relationships are seen in general between ENSO and the maximum daily total precipitation over the SE and NE, in particular in the Philippines data. Over NE, the strongest positive correlation is observed during the winter monsoon period (DJF), that is, a very high possibility for an increase in the maximum daily rainfall total over this region is expected with La Niña episodes during this season. We generally expect an increase in the maximum daily rainfall total over NE with La Niña episodes in all, except the June–August (JJA) seasons. Over NW, the effect of ENSO is less clear.

An increase in the maximum daily rainfall total over SE with the intensification of the La Niña episodes is seen in all except MAM seasons, where a switch in the relationships (positive to negative) along the western coastal region is observed from DJF to MAM. A coherent positive correlation over SW during the SON season exists, which indicates an increase in the maximum daily rainfall total with La Niña episodes. Positive correlations are reduced during DJF and further more in MAM and limited to the northern parts. There is no consistent relationship during the JJA season over SW.

3.3.2 | Relationship with IOD

The majority of stations (84%) show positive correlations between TN90p and DMI (all correlations are based on synchronous values and no lagged correlations are shown). Figure 7 indicates that in general warmer temperatures are expected in a positive IOD year, that is, when the eastern Indian Ocean is colder than normal. All, except one, stations in the southern subregions, show positive correlations ($.2 < \rho < .6$) between the indices. A cluster of stations along the

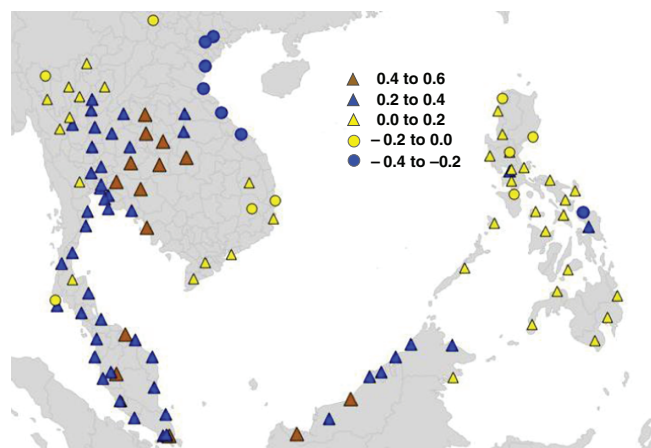


FIGURE 7 Correlation between annual mean (from July to June) of TN90p and the IOD

eastern coast of NW indicate an increase in the frequency of warm nights with the intensification of negative IOD years ($-.4 < \rho < -.2$), and the relationship is weaker over NE. Strongest relationships with IOD are expected in the regions directly bordering the Indian Ocean. It is interesting to note the area on the east coast of Vietnam showing strong negative and spatially consistent correlation for annual values indicating that positive IOD years lead to colder temperatures along this stretch of the Vietnam coast in opposition to the surrounding area inland.

When compared with the temperature index, we see a weaker correlation between the maximum daily rainfall total and the DMI. We observed only two stations with $\rho > .4$ and $\rho < -.4$, respectively (Figure 8). Apart from a number of stations over NE and along the eastern coast of SW indicating an increase in the maximum daily rainfall total with the intensification of negative IOD years ($-.4 < \rho < -.2$), we see mixed relationships over other subregions.

When considering the seasonal cycle, we see weaker relationships between the climate indices and the IOD than we did with the ENSO (not shown). IOD episodes have the strongest influence on the occurrence of warm nights over southern subregions during the DJF season. This is particularly evident over SW and SE. The IOD has least influence on temperatures in the region during the MAM season.

We observe positive correlations in all seasons over SW in TN90p. An increase in the number of warm nights is also observed during a positive IOD year in all seasons except MAM over SE. Over NW, an increase in the number of warm nights is observed with the strengthening of positive IOD year in all seasons with exception of a small group of stations in the north of Thailand during DJF. Results for NE are again mixed, with a more coherent negative relationship in DJF than in SEA. An increase in warm nights during positive IOD events is however expected in JJA. Being furthest from the Indian Ocean temperature indices in NE are less likely to be influenced by the IOD, and the results here

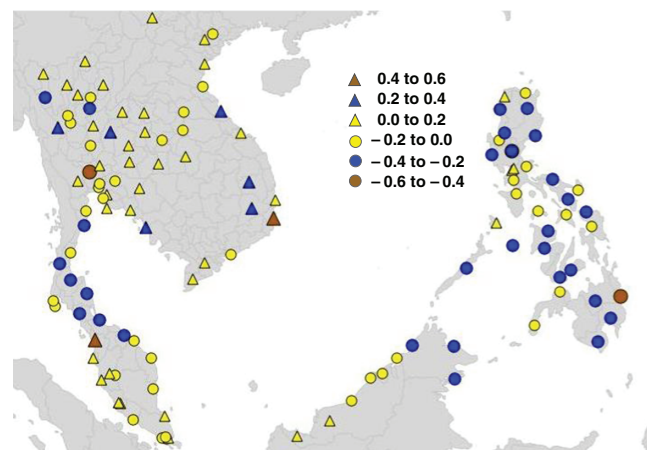


FIGURE 8 Correlation between annual mean (from July to June) of RX1day and the IOD

TABLE 6 Modelled trends in temperature indices for the period 1972–2001. Observed trends are given in brackets for comparison; trend significant at the 5% level are highlighted in bold

Index	SEA	NW	NE	SE	SW	Units/decade
TX90p	2.31 (3.32)	0.82 (4.40)	4.42 (1.73)	3.22 (1.23)	2.02 (4.73)	Percentage of days
TX10p	-1.42 (-1.83)	0.6 (-2.21)	-2.80 (-1.22)	-3.51 (-1.00)	-2.03 (-2.01)	Percentage of days
TN90p	6.32 (4.70)	3.62 (3.72)	8.53 (3.71)	7.50 (6.14)	7.82 (6.23)	Percentage of days
TN10p	-4.91 (-4.40)	-2.23 (-3.22)	-5.51 (-3.23)	-6.92 (-6.43)	-7.52 (-5.91)	Percentage of days
TXx	0.06 (0.11)	-0.02 (0.12)	0.15 (0.0007)	0.16 (0.07)	-0.03 (0.17)	°C
TXn	0.01 (0.18)	-0.14 (0.09)	0.24 (0.28)	0.15 (0.21)	-0.06 (0.20)	°C
TNx	0.2 (0.18)	0.09 (0.11)	0.23 (0.05)	0.24 (0.31)	0.26 (0.33)	°C
TNn	0.3 (0.68)	0.14 (0.97)	0.47 (0.51)	0.34 (0.55)	0.35 (0.59)	°C
DTR	-0.2 (-0.14)	-0.23 (-0.08)	-0.15 (-0.15)	-0.12 (-0.28)	-0.27 (-0.17)	°C

may in fact be a manifestation of ENSO and IOD co-evolution.

As with the annual totals the seasonal relationship (not shown) with precipitation is much less spatially coherent than with ENSO. Strongest relationships are seen in DJF and MAM, with some indication of a negative relationship over the Philippines in DJF, and a positive relationship over much of Thailand in MAM. Relationships are weakest in SON, and in SE and SW in JJA.

3.4 | Representation of extremes in a RCM

In order to assess how useful modelled climate projections for the future are, we need to know how well the model performs in a historical context. By comparing indices calculated from a RCM run (Met Office Hadley Centre HadRM3P) with the station data over the same period, we can get an estimate of our confidence in the model. Table 6 presents the trends in model data compared to station data trends from 1972 to 2001. Note that this preliminary investigation has been achieved using a single RCM simulation, preventing any possibility to assess internally generated variability; results may also be different if a different RCM is used or if the same RCM is driven by a different reanalysis.

3.4.1 | Representation of temperature extremes

The model reproduces well the inter-annual variability of all temperature indices, with Pearson's coefficient greater than .8 except for TXn (not shown). Indices for warm and cool days, warm and cool nights (Tx90, Tx10, Tn90 and Tn10) are closely related across the region. Trends in TX90p and TX10p are well reproduced for the region as a whole; however, there are subregional differences, with trends overestimated on the whole in NE and SE and underestimated in NW and SW, particularly for TX90p (Table 6). TN90p and TN10p capture the significant trends found in the station data, although again slightly overestimate the trends in the eastern half of the region.

The more extreme maximum temperature indices are well represented in the model for both TNn and TNx. As with the observations, trends in the model TXx and TXn

show low significance; subregional differences are however well correlated with the station results. The result of this is an overall underestimate of the DTR (Figure 9) which in magnitude is particularly poor for SE. In contrast the trend in DTR is well reproduced by the model, for the region as a whole and in particular for NE, albeit with a strong underestimation of the DTR absolute value by the model. The existing literature (see, e.g., Stone and Weaver, 2002) suggests that trends in DTR are not well represented in models in general; this study results suggest otherwise. The trends apparent in the model (which does not contain land use change or urbanization) also provide added confidence that observed trends in DTR, as shown in Figure 9, are not due to urban influences.

3.4.2 | Representation of precipitation extremes

Grid box averages of the model are not expected to capture the exact magnitude of extreme values found in station point data. This is particularly true for rainfall extremes as precipitation tends to be more spatially and temporally heterogeneous. This means a lower level of agreement between station and model data is understandable. In addition, it is worth noting that the model will underestimate the magnitude of threshold-based indices R40mm and R20mm because it uses an area average rather than a point. This will have a compounded effect on correlation coefficients by affecting the largest (most extreme values) the most. Therefore, we focus here on whether the model is able to capture spatial and temporal trends in precipitation extremes.

The trends in precipitation totals (PRCPTOT) are overestimated in all regions, and this is a feature of most of the precipitation indices (Table 7). The overestimation is significant, across the region, it is more than threefold what has been observed and equal to about 10% of the mean rainfall. R99, R95, RX1day and RX5day all show the model consistently overestimating station data trends. This is particularly true for NW and SW. However, importantly, where the observed data indicated a statistically significant trend, the model also indicates a statistically significant trend of the correct sign. In particular, SDII is represented well, and the statistically significant negative trends are captured,

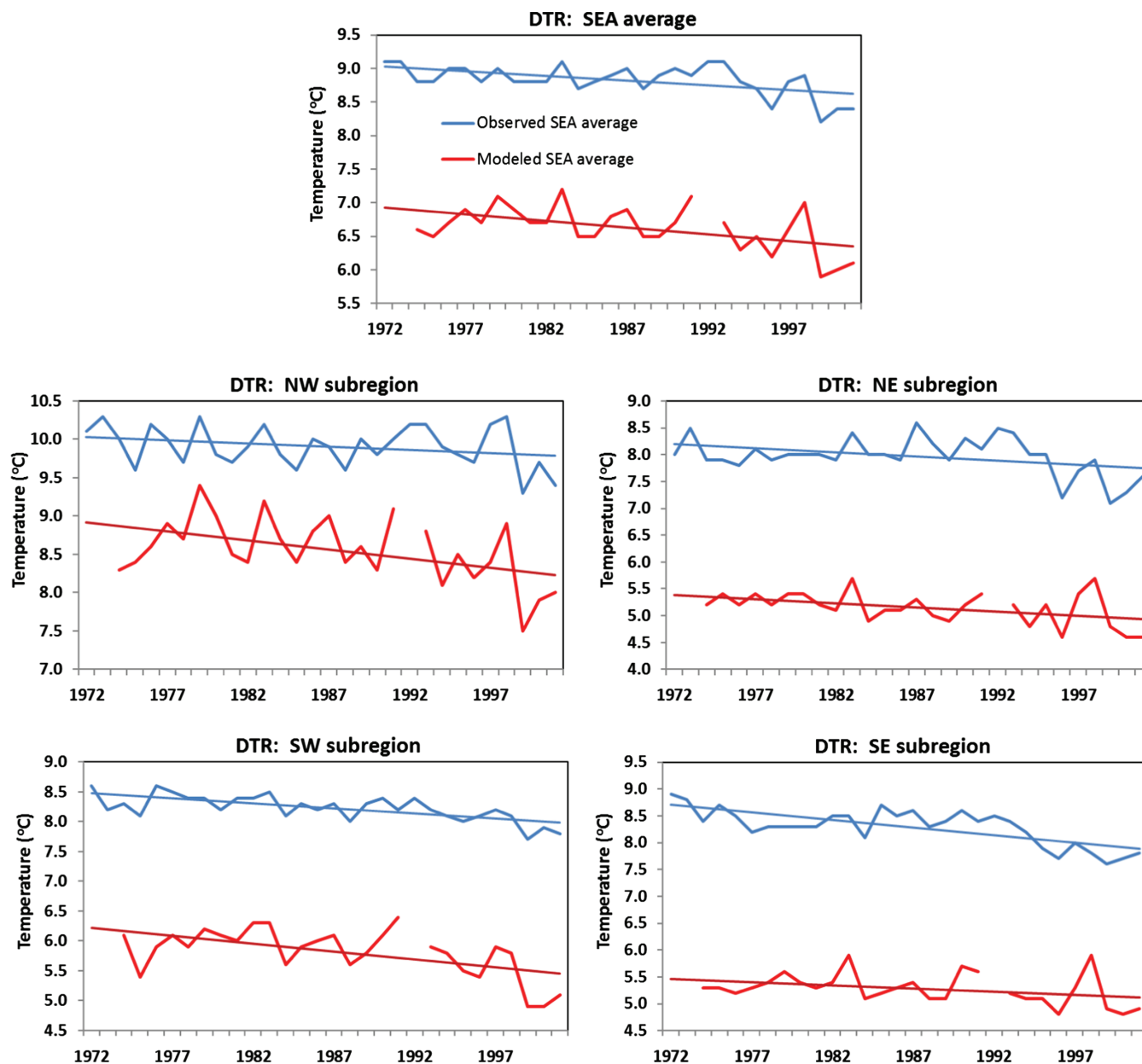


FIGURE 9 Regional (top) and subregional (bottom four panels) time series (1972–2001) for DTR (units: °C). Straight line indicates ordinary least squares fit, model results are in red and station data in blue

TABLE 7 Modelled trends in precipitation indices for the period 1972–2001. Observed trends are given in brackets for comparison; trend significant at the 5% level are highlighted in bold

Index	SEA	NW	NE	SE	SW	Units/decade
PRCPTOT	182.0 (56.7)	142.9 (17.3)	156.3 (74.4)	205.0 (31.7)	254.9 (104.9)	mm
SDII	-0.2 (-0.14)	-0.23 (-0.08)	-0.15 (-0.15)	-0.12 (-0.28)	-0.27 (-0.17)	mm/day
CDD	-3.0 (-0.8)	-3.4 (1.9)	-4.0 (-2.4)	-1.0 (-1.2)	-2.8 (-2.8)	Days
CWD	3.5 (-0.2)	2.8 (-0.06)	4.4 (-0.2)	2.3 (-0.1)	4.3 (-0.2)	Days
RX5day	15.6 (-0.01)	19.4 (5.1)	7.5 (-8.9)	17.0 (-8.4)	16.3 (2.8)	mm
RX1day	7.4 (1.6)	10.4 (3.4)	-1.6 (-3.1)	10.6 (-2.5)	9.0 (4.1)	mm
R99p	0.009 (0.002)	0.01 (0.002)	-0.005 (0.001)	0.01 (0.003)	0.02 (0.004)	mm
R95p	0.03 (0.006)	0.03 (0.007)	0.01 (0.0002)	0.02 (0.004)	0.04 (0.01)	mm
R40mm	0.66 (0.59)	0.67 (0.3)	0.65 (0.93)	0.7 (0.2)	0.53 (0.84)	Days
R20mm	3.1 (1.0)	2.7 (0.5)	2.6 (1.4)	3.2 (0.9)	4.3 (1.7)	Days

although spatial distribution is not quite correct. There are some other variations in the subregional trends (Table 7); for instance, the significant negative trends found in the SE and NE (Table 7) are not represented so well in the model. It is also interesting to note that in some instances the model produces extreme rainfall trends where there are no significant trends evident in the station data, for instance in RX5day and R95p, R20mm and R40mm (Table 7). No significant trends are found in the CDD apart for SW which is captured by the model as are other subregional variation except for NW. As with other indices, trends in CWD (Table 7) are overestimated across the region. For SEA, NW and NE the model produces significant increasing trends, whereas the station data show insignificant decreasing trends.

4 | DISCUSSION AND CONCLUSIONS

In this article we have presented the results from a new and updated data set of climate extremes in six countries in SEA. The data set presents indices calculated from station data not used in previous studies, which have been subject to consistent quality control procedure and allow up-to-date assessment of temperature and precipitation extremes.

Our findings complement previous studies by Manton *et al.* (2001) and Caesar *et al.* (2011), providing further evidence of increases in temperature extremes. Statistically significant trends are found across the region and are particularly strong in the SW part of SEA. As with previous studies (Alexander *et al.*, 2006; Klein Tank *et al.*, 2006; Choi *et al.*, 2009) we find that the increasing trend in warm nights is the most spatially coherent index, although the trends found in this study tend to be greater than those found previously. As with Caesar *et al.* (2011) we find that trends in precipitation indices are less coherent than temperature trends. However, results shown here give greater evidence of increasing trends both at a regional and subregional scale than found previously. In general, and in agreement with the global results (Alexander *et al.*, 2006; Donat *et al.*, 2013) the trend is towards wetter conditions.

We also considered the relationship between extremes indices and two modes of internal climate variability known to influence the climate of this region. Our results show particularly strong correlations between indices and ENSO, with the strongest relationships in precipitation over the Philippines. Relationships across the region with IOD are less coherent; however, the data here show the strongest influence in regions bordering the Indian Ocean.

By comparing the trends in indices from station data with those from the Met Office Hadley Centre RCM (HadRM3P), we find that temperature trends are very well simulated by the model, and as we expect, due to the influences of ENSO and IOD (in both the observations and model boundary conditions), the inter-annual variability in

this region is strongly correlated with the station data. Previous analysis (Intergovernmental Panel on Climate Change, 2013) has found higher uncertainty in model projections of precipitation than temperature; this has been found true also for simulating present-day extremes, particularly in the Tropics and subtropics (Kharin *et al.*, 2007). This is also evident here, while precipitation extremes are not well captured by the model, majority of trends are overestimated. At subregions level, results are mixed.

The results presented here are part of an ongoing effort to provide more useful and robust records of the current climate, as well as assess influences of the future climate on extreme weather conditions. The new analysis performed as part of this workshop and updated results from previous workshops will allow decision makers to plan adaptation structures that will increase resilience to extreme events that we have observed to be increasing in frequency (i.e., both warm days and warm nights are increasing and the latter are increasing faster, similarly extreme rainfall are also increasing) and are predicted to become more frequent or intense, as well as maximize any benefits that may result from trends such as a reduction in extreme cold. The investigation of extremes as simulated by the RCM suggests that this will be a useful tool when considering future changes to temperature extremes, although important biases were noted and would need to be taken in consideration. In some smaller regions information about future precipitation extremes can start to be gleaned, although further investigation using a range of regional-scale models, and investigation of what is driving the model performances noted here would be worthwhile.

ACKNOWLEDGEMENTS

The authors would like to acknowledge the National Environment Agency (NEA) Singapore for funding the Regional Workshop for Southeast Asia Climate Analysis and Modelling Study in May 2011 and for funding the participants from ASEAN Met Services. The authors would also like to thank the Met Office Hadley Centre regional climate modelling team for conducting the workshop. Dr Muhammad Hassim (MSS) generated the first figure.

ORCID

B. Timbal  <http://orcid.org/0000-0002-7342-8994>

REFERENCES

- Alexander, L.V. and Arblaster, J.M. (2009) Assessing trends in observed and modelled climate extremes over Australia in relation to future projections. *International Journal of Climatology*, 29, 417–435.
- Alexander, L.V. and Arblaster, J.M. (2017) Historical and projected trends in temperature and precipitation extremes in Australia in observations and CMIP5. *Weather and Climate Extremes*, 15, 34–56. <https://doi.org/10.1016/j.wace.2017.02.001>.
- Alexander, L.V., Uotila, P. and Nicholls, N. (2009) Influence of sea surface temperature variability on global temperature and precipitation extremes.

- Journal of Geophysical Research*, 114, D18116. <https://doi.org/10.1029/2009JD012301>.
- Alexander, L.V., Zhang, X., Peterson, T.C., Caesar, J., Gleason, B., Tank, A.M. G.K., Haylock, M., Collins, D., Trewin, B., Rahimzadeh, F., Tagipour, A., Ambenje, P., Kumar, K.R., Revadekar, J., Griffiths, G., Vincent, L., Stephenson, D.B., Burn, J., Aguilari, E., Brunet, M., Taylor, M., New, M., Zhai, P., Rusticucci, M. and Vazquez-Aguirre, J.L. (2006) Global observed changes in daily climate extremes of temperature and precipitation. *Journal of Geophysical Research*, 111, D05109. <https://doi.org/10.1029/2005JD006290>.
- Allan, R.J., Chambers, D., Drosowsky, W., Hendon, H., Latif, M., Nicholls, N., Smith, I., Stone, R.C. and Turre, Y. (2001) Is there an Indian Ocean Dipole and is it independent of the El Niño-Southern Oscillation? *CLIVAR Exchanges*, 63(21), 18–22.
- Behera, S.K., Luo, J.J., Masson, S., Rao, S.A. and Sakuma, H. (2005) A CGCM study on the interaction between IOD and ENSO. *Journal of Climate*, 19, 1688–1705.
- Bhaskaran, B., Jones, R.G., Murphy, J.M. and Noguer, M. (1996) Simulations of the Indian summer monsoon using a nested regional climate model: domain size experiments. *Climate Dynamics*, 12, 573–587.
- Caesar, J., Alexander, L.V., Trewin, B., Tse-ring, K., Sorany, L., Vuniyayawa, V., Keosavang, N., Shimana, A., Htay, M.M., Karmacharya, J., Jayasinghearachchi, D.A., Sakkamart, J., Soares, E., Hung, L.T., Thuong, L.T., Hue, C.T., Dung, N.T.T., Hung, P.V., Cuong, H. D., Cuong, N.M. and Sirabaha, S. (2011) Changes in temperature and precipitation extremes over the Indo-Pacific region from 1971 to 2005. *International Journal of Climatology*, 31(6), 791–801.
- Chan, J.C.L. (2005) Interannual and interdecadal variations of tropical cyclone activity over the western North Pacific. *Meteorology and Atmospheric Physics*, 89, 143–152.
- Chan, J.C.L. and Shi, J.E. (1996) Long-term trends and interannual variability in tropical cyclone activity over the western North Pacific. *Geophysical Research Letters*, 23, 2765–2767.
- Chang, C.P., Wang, Z., Ju, J. and Li, T. (2003) On the relationship between western Maritime Continent rainfall and ENSO during northern winter. *Journal of Climate*, 17, 665–672.
- Choi, G., Collins, D., Ren, G., Trewin, B., Baldi, M., Fukuda, Y., Afzaal, M., Pianmana, T., Gomboluudev, P., Huong, P.T.T., Lias, N., Kwon, W.-T., Boo, K.-O., Cha, Y.-M. and Zhou, Y. (2009) Changes in means and extreme events of temperature and precipitation in the Asia-Pacific network region, 1955–2007. *International Journal of Climatology*, 29, 1906–1925.
- Diaz, H.F., Hoerling, M.P. and Eischeid, J.K. (2001) ENSO variability, teleconnections and climate change. *International Journal of Climatology*, 21, 1845–1862. <https://doi.org/10.1002/joc.631>.
- Donat, M.G., Alexander, L.V., Yang, H., Durre, I., Vose, R., Dunn, R.J.H., Willett, K.M., Aguilar, E., Brunet, M., Caesar, J., Hewitson, B., Jack, C., Klein Tank, A.M.G., Kruger, A.C., Marengo, J., Peterson, T.C., Renom, M., Oria Rojas, C., Rusticucci, M., Salinger, J., Elrayah, A.S., Sekele, S.S., Srivastava, A.K., Trewin, B., Villarroya, C., Vincent, L.A., Zhai, P., Zhang, X. and Kitching, S. (2013) Updated analyses of temperature and precipitation extreme indices since the beginning of the twentieth century: the HadEX2 dataset. *Journal of Geophysical Research: Atmospheres*, 118, 2098–2118. <https://doi.org/10.1002/jgrd.50150>.
- Easterling, D.R., Diaz, H.F., Douglas, A.V., Hogg, W.D., Kunkel, K.E., Rogers, J.C. and Wilkinson, J.F. (1999) Long-term observations for monitoring extremes in the Americas. *Climatic Change*, 42, 285–308.
- Gervais, M., Gyakum, J.R., Atallah, E., Tremblay, L.B. and Neale, R.B. (2014) How well are the distribution and extreme values of daily precipitation over North America represented in the community climate system model? A comparison to reanalysis, satellite, and gridded station data. *Journal of Climate*, 27, 5219–5239. <https://doi.org/10.1175/JCLI-D-13-00320.1>.
- Goh, A.Z.C. and Chan, J.C.L. (2010) Interannual and interdecadal variations of tropical cyclone activity in the South China Sea. *International Journal of Climatology*, 30, 827–843.
- Haylock, M.R., Hofstra, N., Klein Tank, A.M.G., Klok, E.J., Jones, P.D. and New, M. (2008) A European daily high-resolution gridded dataset of surface temperature and precipitation. *Journal of Geophysical Research: Atmospheres*, 113, D20119. <https://doi.org/10.1029/2008JD10201>.
- Herrera, S., Fita, L., Fernández, J. and Gutiérrez, J.M. (2010) Evaluation of the mean and extreme precipitation regimes from the ENSEMBLES regional climate multimodel simulations over Spain. *Journal of Geophysical Research*, 115, D21117. <https://doi.org/10.1029/2010JD013936>.
- Ho, C.H., Baik, J.J., Kim, J.H., Gong, D.Y. and Sui, C.H. (2004) Interdecadal changes in summertime typhoon tracks. *Journal of Climate*, 17, 1767–1776.
- Hofstra, N., Haylock, M., New, M. and Jones, P.D. (2009) Testing E-OBS European high-resolution gridded data set of daily precipitation and surface temperature. *Journal of Geophysical Research: Atmospheres*, 114, D21.
- Intergovernmental Panel on Climate Change. (2007) *Climate Change 2007: the physical science basis*. In: Solomon, S., Qin, D., Manning, M., Chen, Z., Marquis, M., Averyt, K.B., Tignor, M. and Miller, H.L. (Eds.) *Contribution of Working Group I to the Fourth Assessment Report of the Intergovernmental Panel on Climate Change*. Cambridge, NY: Cambridge University Press.
- Intergovernmental Panel on Climate Change. (2012) *Managing the risks of extreme events and disasters to advance climate change adaptation*. In Field, C.B., Barros, V., Stocker, T.F., Qin, D., Dokken, D.J., Ebi, K.L., Mastrandrea, M.D., Mach, K.J., Plattner, G.-K., Allen, S.K., Tignor, M., and Midgley, P.M. (Eds.) *A Special Report of Working Groups I and II of the Intergovernmental Panel on Climate Change*. Cambridge, NY: Cambridge University Press. pp. 582.
- Intergovernmental Panel on Climate Change. (2013) *Climate change 2013: the physical science basis*. In: Stocker, T. F., Qin, D., Plattner, G.-K., Tignor, M., Allen, S. K., Boschung, J., Nauels, A., Xia, Y., Bex, V. and Midgley, P. M. (Eds.) *Contribution of Working Group I to the Fifth Assessment Report of the Intergovernmental Panel on Climate Change*. Cambridge, NY: Cambridge University Press. pp. 1535.
- Jones R.G., M. Noguer, D.C. Hassell, D. Hudson, S.S. Wilson, G.J. Jenkins and J.F.B. Mitchell (2004) *Generating High Resolution Climate Change Scenarios using PRECIS*. Exeter: Met office Hadley Centre. pp. 40.
- Ju, J. and Slingo, J. (1995) The Asian summer monsoon and ENSO. *Quarterly Journal of Royal Meteorological Society*, 121, 1133–1168. <https://doi.org/10.1002/qj.49712152509>.
- Katz, R.W. and Brown, B.G. (1992) Extreme events in a changing climate: variability is more important than averages. *Climatic Change*, 21, 289–302.
- Kenyon, J. and Hegerl, G.C. (2008) Influence of modes of climate variability on global temperature extremes. *Journal of Climate*, 21, 3872–3889. <https://doi.org/10.1175/2008JCLI2125.1>.
- Kenyon, J. and Hegerl, G.C. (2010) Influence of modes of climate variability on global precipitation extremes. *Journal of Climate*, 23, 6248–6262. <https://doi.org/10.1175/2010JCLI3617.1>.
- Kharin, V.V., Zwiers, F.W., Zhang, X. and Hegerl, G.C. (2007) Changes in temperature and precipitation extremes in the IPCC ensemble of global coupled model simulations. *Journal of Climate*, 20, 1419–1444.
- Klein Tank, A.M.G., Peterson, T.C., Quadir, D.A., Dorji, S., Zou, X., Tang, H., Santhosh, K., Joshi, U.R., Jaswal, A.K., Kolli, R.K., Sikder, A.B., Deshpande, N.R., Revadekar, J.V., Yeleuova, K., Vandasheva, S., Faleyeva, M., Gomboluudev, P., Budhathoki, K.P., Hussain, A., Afzaal, M., Chandrapala, L., Anvar, H., Amanmurad, D., Asanova, V.S., Jones, P.D., New, M.G. and Spektorman, T. (2006) Changes in daily temperature and precipitation extremes in central and South Asia. *Journal of Geophysical Research: Atmospheres*, 111, D16105. <https://doi.org/10.1029/2005JD006316>.
- Le Loh, J., Tangang, F., Juneng, L., Hein, D. and Lee, D.-I. (2016) Projected rainfall and temperature changes over Malaysia at the end of the 21st century based on PRECIS modelling system. *Asia-Pacific Journal of Atmospheric Sciences*, 52, 191–208.
- Liu, K.S. and Chan, J.C. (2003) Climatological characteristics and seasonal forecasting of tropical cyclones making landfall along the South China coast. *Monthly Weather Review*, 131(8).
- Liu, K.S. and Chan, J.C.L. (2008) Interdecadal variability of western North Pacific tropical cyclone tracks. *Journal of Climate*, 21, 4464–4476.
- Manton, M.J., Della-Marta, P.M., Haylock, M.R., Hennessy, K.J., Nicholls, N., Chambers, L.E., Collins, D.A., Daw, G., Finet, A., Gunawan, D., Inape, K., Isobe, H., Kestin, T.S., Lefale, P., Leyu, C.H., Lwin, T., Maitrepierre, L., Ouprasitwong, N., Page, C.M., Pahalad, J., Plummer, N., Salinger, M.J., Suppiah, R., Tran, V.L., Trewin, B., Tibig, I. and Yee, D. (2001) Trends in extreme daily rainfall and temperature in Southeast Asia and the South Pacific: 1916–1998. *International Journal of Climatology*, 21, 269–284.
- Meehl, G.A., Arblaster, J.M. and Tebaldi, C. (2007) Contributions of natural and anthropogenic forcing to changes in temperature extremes over the United States. *Geophysical Research Letters*, 34, L19709. <https://doi.org/10.1029/2007GL030948>.

- Nicholls, N. (1981) Air–sea interaction and possibility of long-range weather prediction in the Indonesian Archipelago. *Monthly Weather Review*, 109, 2435–2443.
- Peterson, T.C. and Manton, M.J. (2008) Monitoring changes in climate extremes: a tale of international collaboration. *Bulletin of the American Meteorological Society*, 89, 1266–1271. <https://doi.org/10.1175/2008BAMS2501.1>.
- Redmond, G., Hodges, K.I., Mcsweeney, C., Jones, R. and Hein, D. (2015) Projected changes in tropical cyclones over Vietnam and the South China Sea using a 25 km regional climate model perturbed physics ensemble. *Climate dynamics*, 45, 1983–2000.
- Saji, N.H. and Yamagata, T. (2003) Possible impacts of Indian Ocean Dipole mode events on global climate. *Climate Research*, 25, 151–169.
- Sillman, J. and Roeckner, E. (2008) Indices for extreme events in projections of anthropogenic climate change. *Climatic Change*, 86, 83–104.
- Stone, D. and Weaver, A.J. (2002) Daily maximum and minimum temperature trends in a climate model. *Geophysical Research Letters*, 29, 1356. <https://doi.org/10.1029/2001GL014556>.
- Tangang, F.T. and Juneng, L. (2004) Mechanisms of Malaysia rainfall anomalies. *Journal of Climate*, 17, 3616–3622.
- Turner, A.G., Inness, P.M. and Slingo, J.M. (2005) The role of the basic state in the ENSO–monsoon relationship and implications for predictability. *Quarterly Journal of the Royal Meteorological Society*, 131, 781–804. <https://doi.org/10.1256/qj.04.70>.
- Uppala, S.M., Kållberg, P.W., Simmons, A.J., Andrae, U., Da Costa Bechtold, V., Fiorino, M., Gibson, J.K., Haseler, J., Hernandez, A., Kelly, G.A., Li, X., Onogi, K., Saarinen, S., Sokka, N., Allan, R.P., Andersson, E., Arpe, K., Balmaseda, M.A., Beljaars, A.C.M., Van De Berg, L., Bidlot, J., Bormann, N., Caires, S., Chevallier, F., Dethof, A., Dragosavac, M., Fisher, M., Fuentes, M., Hagemann, S., Hólm, E., Hoskins, B.J., Isaksen, I., Janssen, P.A.E.M., Jenne, R., McNally, A.P., Mahfouf, J.-F., Morcrette, J.-J., Rayner, N.A., Saunders, R.W., Simon, P., Sterl, A., Trenberth, K.E., Untch, A., Vasiljevic, D., Viterbo, P., Woollen, J. and Woollen, J. (2005) The ERA-40 re-analysis. *Quarterly Journal of the Royal Meteorological Society*, 131, 2961–3012.
- Webster, P.J. and Yang, S. (1992) Monsoon and ENSO: selective interactive systems. *Quarterly Journal of the Royal Meteorological Society*, 118, 877–926.
- Wilson, W., Hassell, D., Hein, D., Wang, C., Tucker, S., Jones, R. and Taylor, R. (2015). *Technical manual for PRECIS: the met office hadley centre regional climate modelling system version 2.0.0*.

How to cite this article: Cheong WK, Timbal B, Golding N, et al. Observed and modelled temperature and precipitation extremes over Southeast Asia from 1972 to 2010. *Int J Climatol*. 2018;38:3013–3027. <https://doi.org/10.1002/joc.5479>